



**In The Name Of God**

**Investigation of Specific Targeting of Triptorelin  
Conjugated Dextran-Coated Magnetite Nanoparticles as a  
Targeted Probe in GnRH+ Cancer Cells in MRI**

**Present By:**

**Maede Khazaei (971824004)**

**Adviser :**

**Dr. Ahmadpour Yazdi**

# List of contents

✓ Article Information .....	3
✓ Journal Information .....	4
✓ Abstract.....	5
✓ Purpose.....	6
✓ Introduction.....	7
✓ Materials & Methods & Results.....	12
✓ Discussion .....	28
✓ Conclusion.....	35
✓ References .....	37

# Article Information

- Author:

Alireza Montazerabadi

Received: 20 January 2021

- University :

Accepted: 6 May 2021

- Mashhad University of Medical Sciences
- Iran University of Medical Sciences


# About the Journal

WILEY






## Editorial Board

### Chief Editor

- **Luc Zimmer** , Université de Lyon - Hospices Civils de Lyon, France

### Associate Editors

- **María L. García-Martín** , BIONAND - Andalusian Centre for Nanomedicine and Biotechnology, Spain
- **Anne Roivainen** , University of Turku, Finland
- **Ralf Schirmacher** , University of Alberta, Canada

WILEY



### Journal metrics

Acceptance rate	58%
Submission to final decision	65 days
Acceptance to publication	40 days
CiteScore	3.200
Impact Factor	1.984

# Abstract

the conjugation of superparamagnetic iron oxide nanoparticles (SPIONs), as tumor-imaging probes for magnetic resonance imaging (MRI), with tumor targeting peptides possesses promising advantages for specific delivery of MRI agents.

# Purpose

Design a targeted contrast agent for MRI based on Fe<sub>3</sub>O<sub>4</sub> nanoparticles conjugated triptorelin (SPION@triptorelin), which has a great affinity to the GnRH receptors.

1. **Synthesized** SPIONs-coated carboxymethyl dextran (SPION@CMD) conjugated triptorelin (SPION@CMD@triptorelin)
2. **Characterized** by DLS, TEM, XRD, FTIR, Zeta, and VSM techniques
3. **Calculated** the relaxivities of synthesized formulations using a 1.5 Tesla clinical magnetic field
4. Estimated quantitative cellular uptake, and cytotoxicity level of them

# Introduction

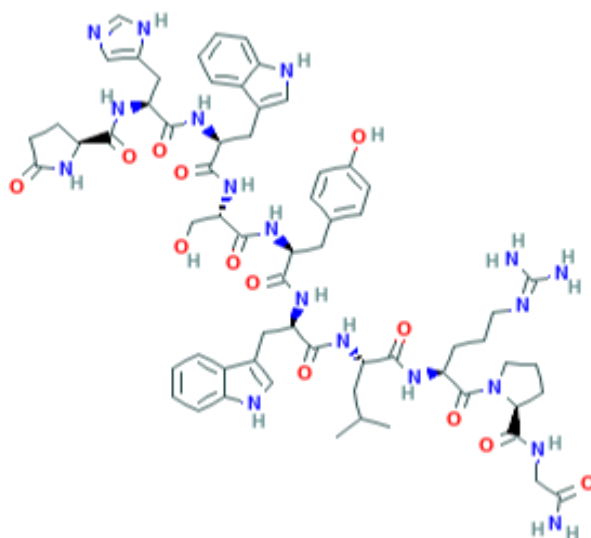
- Cancers are one of the most frequent mortality causes worldwide due to the challenges arising in the diagnosis and clinical management.
- Conventional imaging techniques have played an effective role 😞 they suffer from low specificity.
- Targeted nanomolecular imaging has been proposed as a suitable solution for early detection.
- the detection of cancer based on specific biomarkers or receptors has resulted in substantial improvements in early and specific diagnosis.

- Several methods are used for the diagnosis of various human cancers.
- Imaging tests as a noninvasive way allow examining bones and internal organs.
- the most **common imaging** methods that are used in diagnosing cancer may include a computerized tomography (**CT**) scan, bone scan, **ultrasound**, **X-ray**, scan, and magnetic resonance imaging (**MRI**).
- The superparamagnetic iron oxide nanoparticles (**SPIONs**) are one of the US Food and Drug Administration- (FDA-) approved nanoparticles that are successfully **used as tumor imaging probes for MRI**.
- Used for drug delivery due to their **low toxicity**, **biocompatibility**, and demonstrating a **great potential for theranostic**.



- Coating of SPIONs with organic materials can also improve the colloidal stability.
- Conjugation of SPIONs with tumor targeting represents a promising platform for selective diagnosis of cancer biomarker/receptors and specific delivery of MRI agents.
- The specific binding of a peptide to its receptors (specific ligand-receptor interaction) which are overexpressed in cancer cells, resulting in efficient internalization of SPIONs based on receptor-mediated endocytosis (RME).
- Triptorelin is a synthetic decapeptide gonadotropin-releasing hormone (GnRH) agonis with similar structure to native GnRH and a great affinity to the GnRH receptors.

- **Triptorelin** is a **potent inhibitor** of the synthesis of testosterone (in men), an estrogen (in women) and is utilized to treat advanced prostate cancer and breast cancer.



<https://pubchem.ncbi.nlm.nih.gov/compound/Triptorelin#section=2D-Structure> 2021/June/25

## Triptorelin

Medication

Triptorelin, sold under the brand names Decapeptyl and Gonapeptyl among others, is a medication that acts as an agonist analog of Gonadotropin-releasing hormone, thus reversibly repressing expression of luteinizing hormone and follicle-stimulating hormone.

[Wikipedia](#)

**Molar mass:** 1,311.5 g/mol

**Drug class:** GnRH analogue; GnRH agonist; Antigonadotropin

**ATC code:** L02AE04 (WHO) QH01CA97 (WHO)

**Excretion:** Kidney

**Formula:** C<sub>64</sub>H<sub>82</sub>N<sub>18</sub>O<sub>13</sub>

<https://www.google.com/search?q=triptorelin>  
2021/June/25

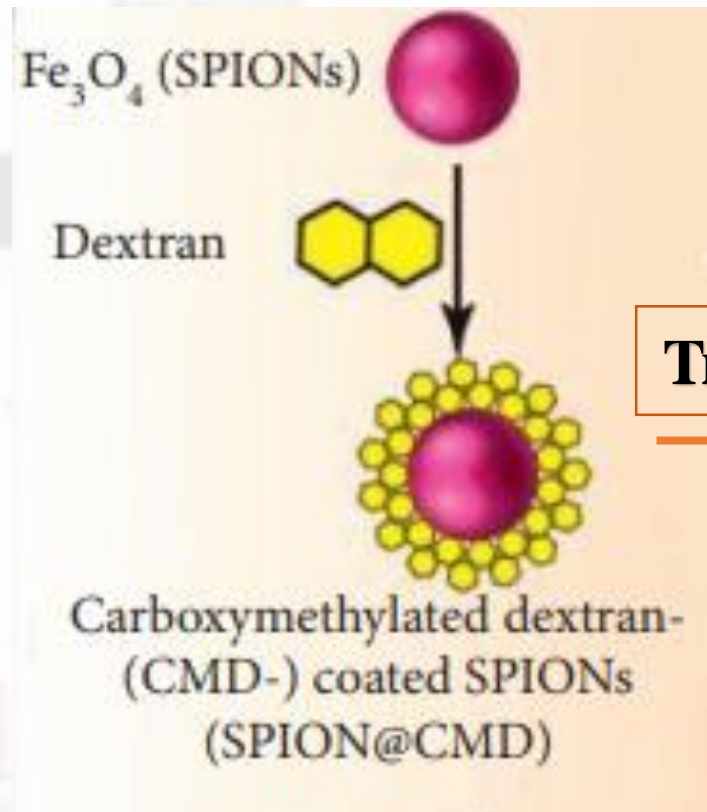
- The conjugation of dextran-coated SPIONs with triptorelin, as a targeting molecule, proper MRI probe for the tumor diagnosis.
- The **triptorelin peptide** was **conjugated** to synthesized **SPION@CMD**.
- the morphological properties and size dispersity of the prepared nanoparticles were assessed.
- The cytotoxicity of formulations was also investigated.
- In order to investigate the potential of synthesized SPION@CMD@triptorelin as a diagnostic nanoprobe, the **MRI technique** was carried out in vitro on **MDA-MB-231** as **GnRH-positive breast cancer cell line**.

# Materials & Methods & Results

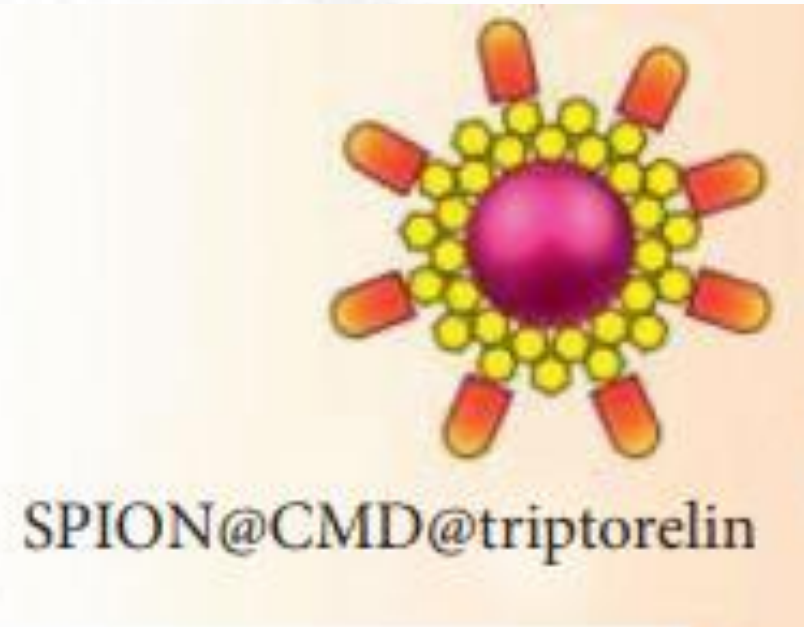
- All materials that were used for synthesis on nanoparticles and other analysis were obtained from Sigma-Aldrich Chemicals, USA.
- Cell culture media (RPMI1640), Fetal Bovine Sera (FBS), Trypsin, and penicillin/streptomycin solution were obtained from Gibco (Darmstadt, Germany)
- MDA-MB-231 cell line was obtained from the National Cell Bank of Iran, Pasteur Institute of Iran.

Step 1

Nanoparticle  
synthesis



**Triptorelin**

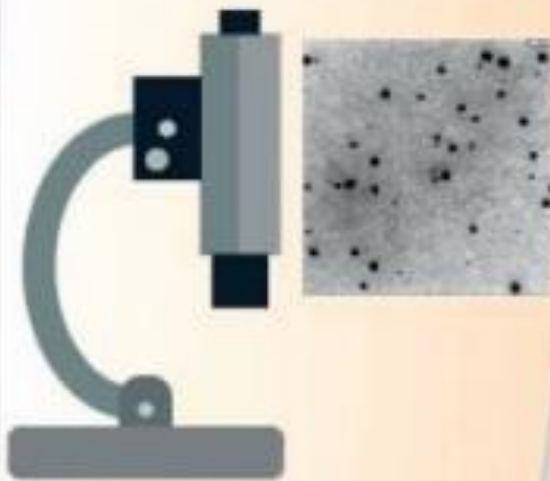




Step 2

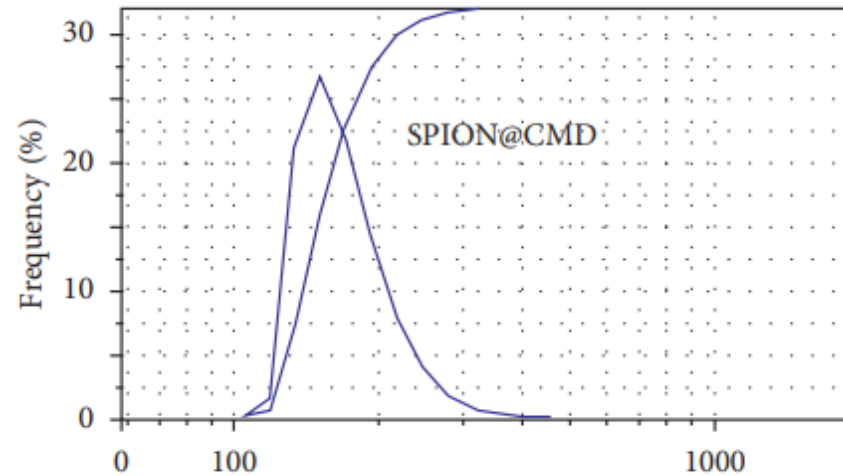


Dynamic light scattering (DLS)

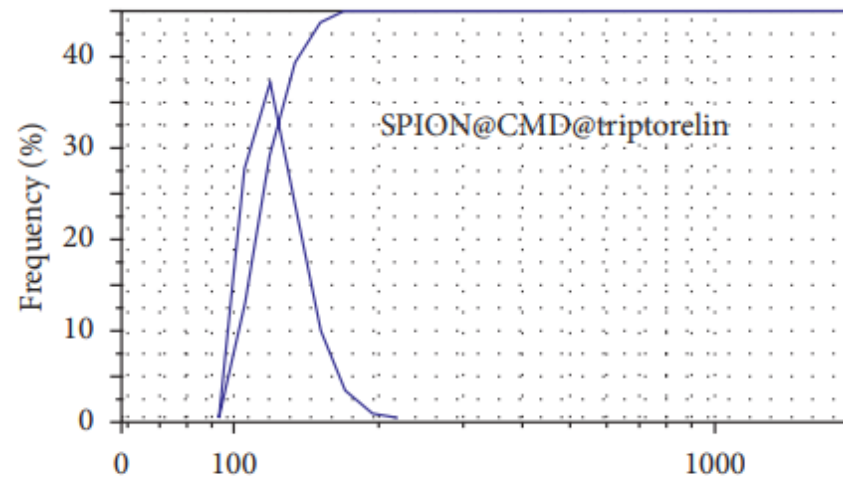


Transmission electron microscopy (TEM)

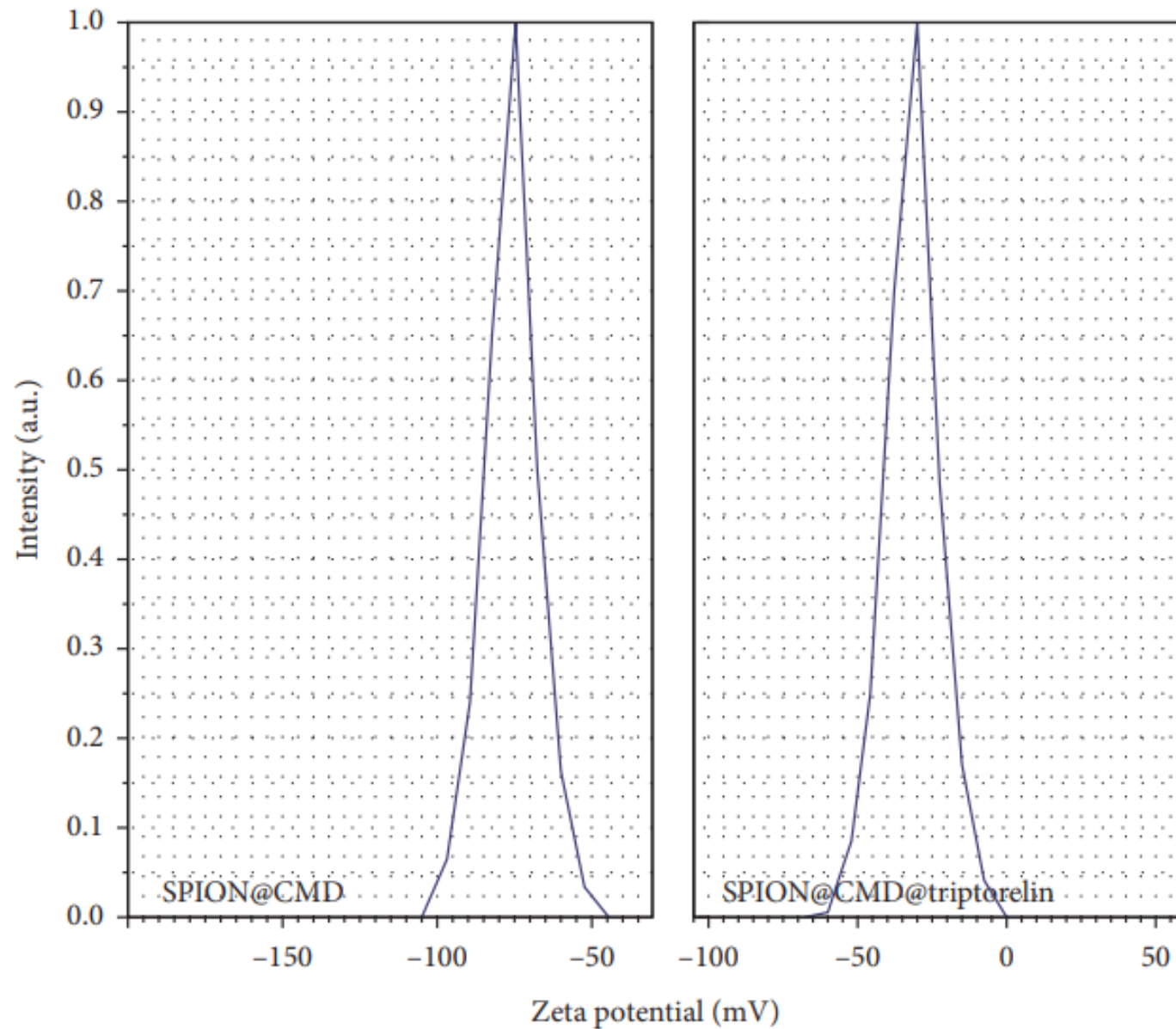
## *DLS Result*



(a)



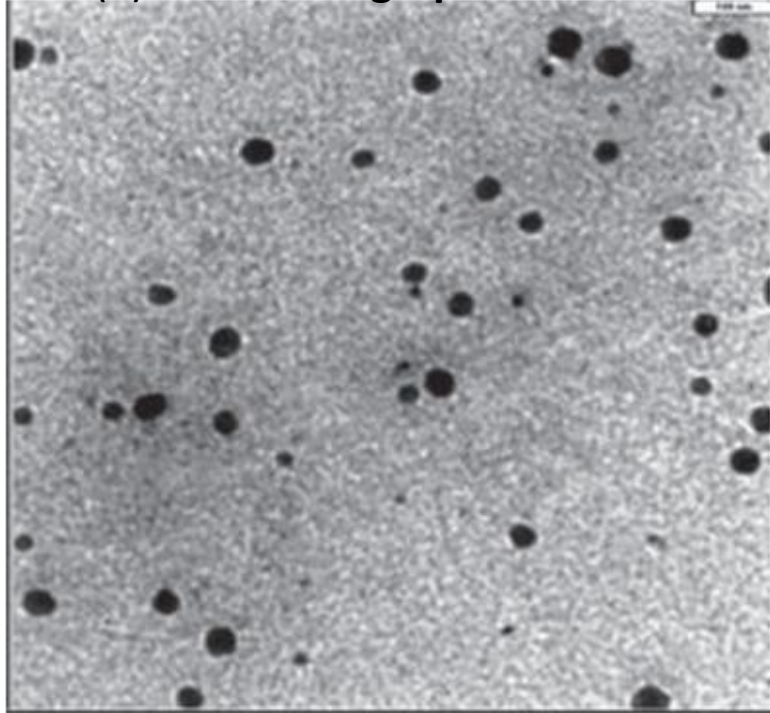
only one peak was observed in both SPION@CMD and SPION@CMD@triptorelin. The highest number of SPION@CMD and SPION@CMD@triptorelin complexes had a diameter of 160 nm and 116 nm, respectively. indicates **narrow particle size distribution** and **monomodal population of the particles** due in part to the contribution of triptorelin with SPIONs.



Zeta potential was measured at  $\sim -72.4$  mV for SPION@CMD and  $\sim -31.5$  mV for SPION@CMD@triptorelin.

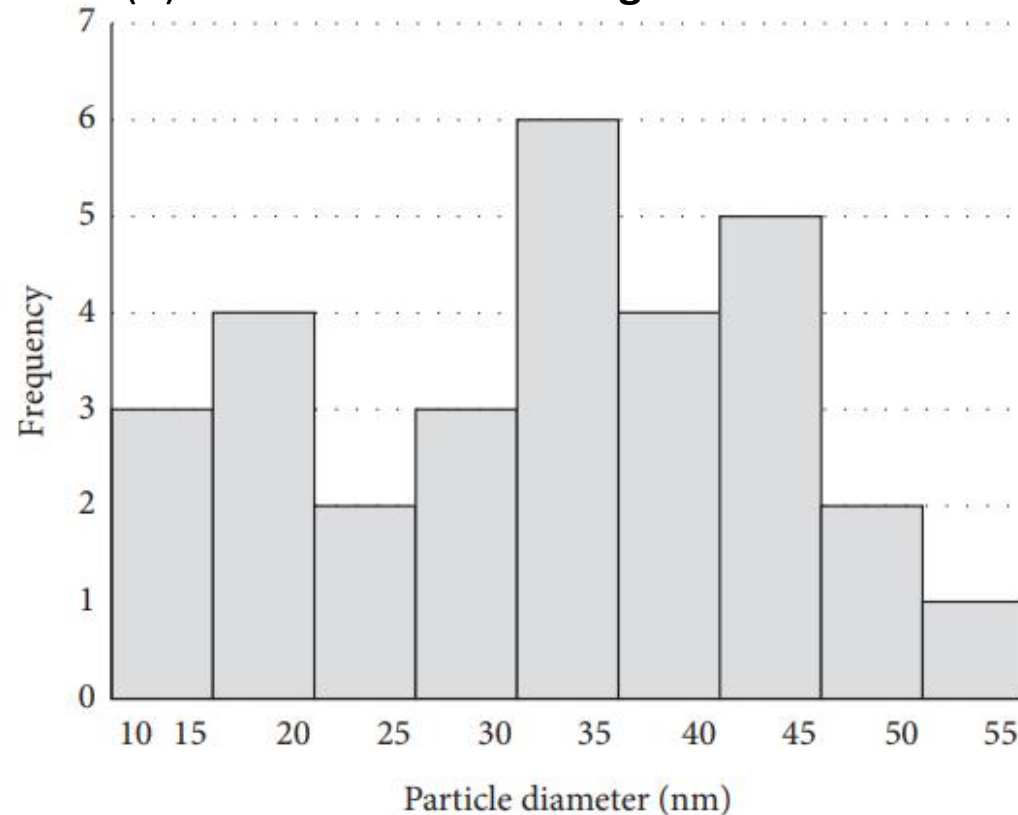
## *TEM Result*

(a) TEM micrograph of SPIONs



(a)

(b) Size distribution histogram of SPIONs

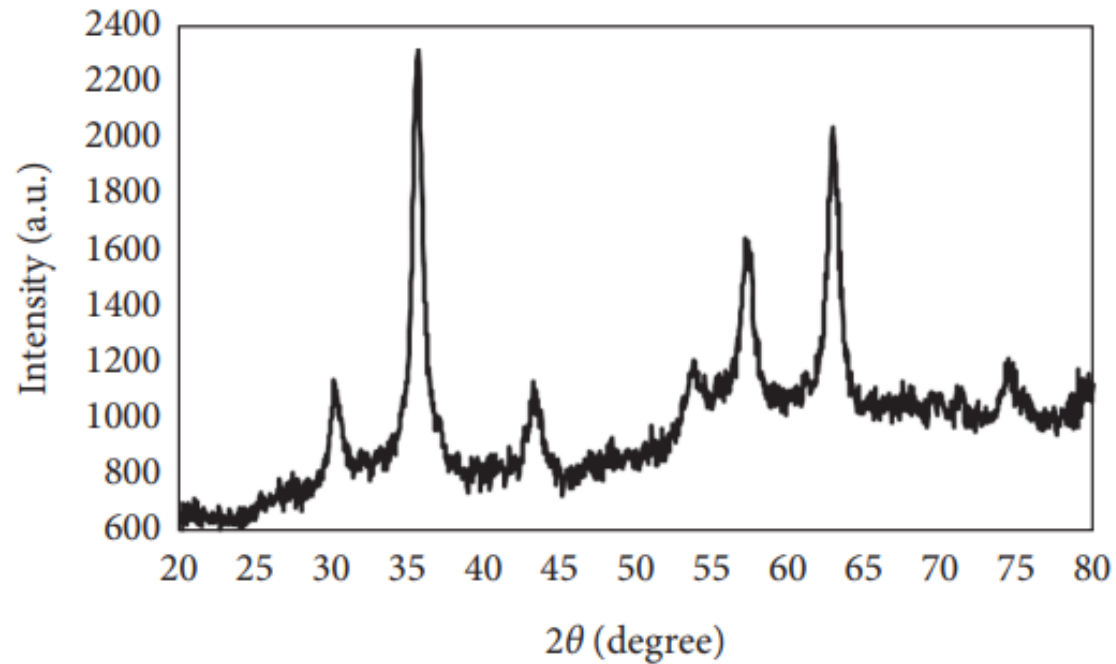


(b)

According to the TEM image, the synthesized SPION@CMD showed a **spherical** and **homogeneous** morphology. the particle size distribution histogram obtained from TEM image revealed that the **largest** number of SPION@CMD nanoparticles had **dimensions between 30 and 45 nm** with an **average size of  $31.35 \pm 11.1$  nm**.

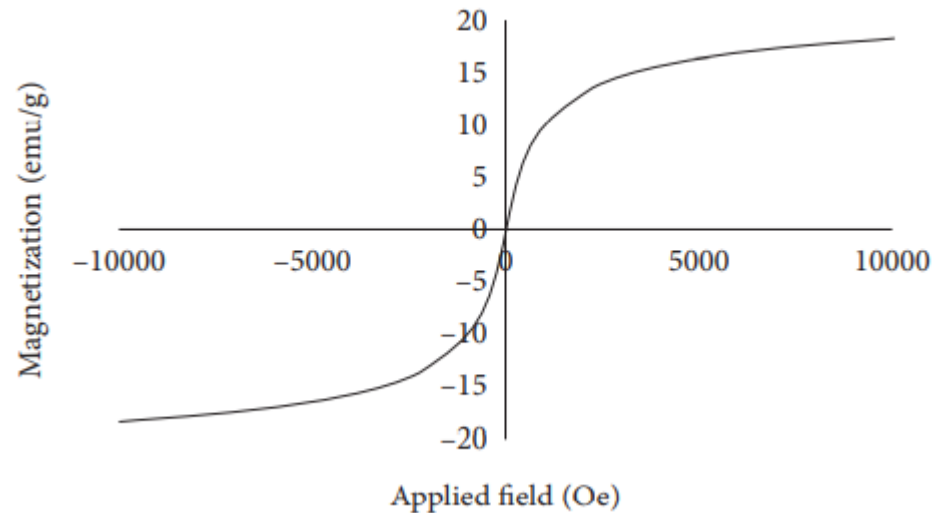


## ***XRD Result***



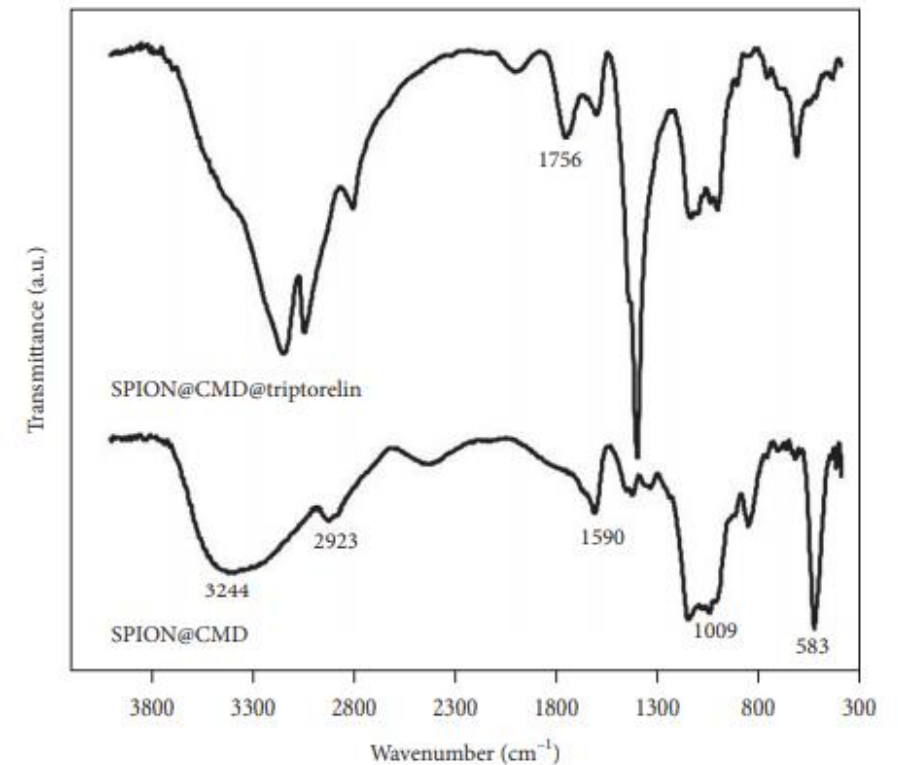
The XRD profile revealed that **maximum XRD peak occurred at  $2\theta$  value of  $35.7^\circ$**  that represented a typical SPION with an interlayer spacing value of 3.83242 Å. The position and relative intensity of all peaks were matched with standard magnetite  $\text{Fe}_3\text{O}_4$  pattern (JCPDS card, file no. 19-0629), indicating that the synthesized nanoparticles are magnetic ( $\text{Fe}_3\text{O}_4$ ) crystals.

## ***VSM Result***



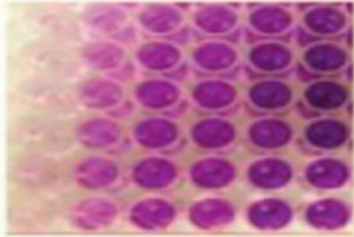
The magnetic characteristics. that nanoparticles possessed superparamagnetism at 27°C with a saturation magnetization ( $M_s$ ) value of 18.26 emu/g

## ***FTIR Result***

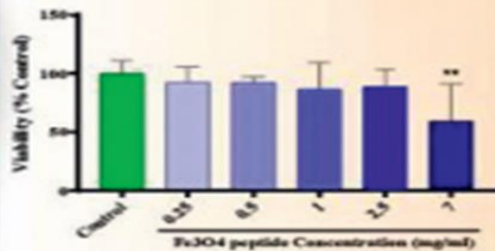


### Step 3

## Cytotoxicity assay

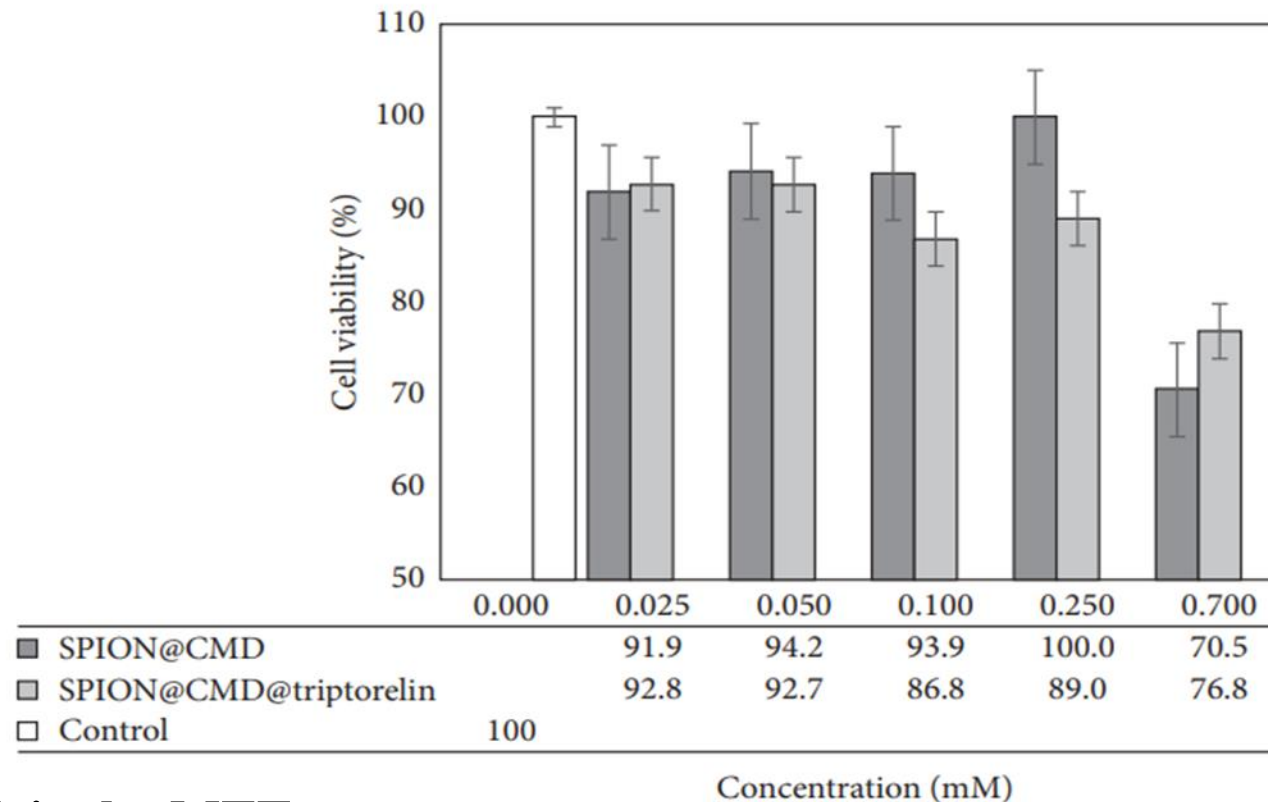


MTT assay



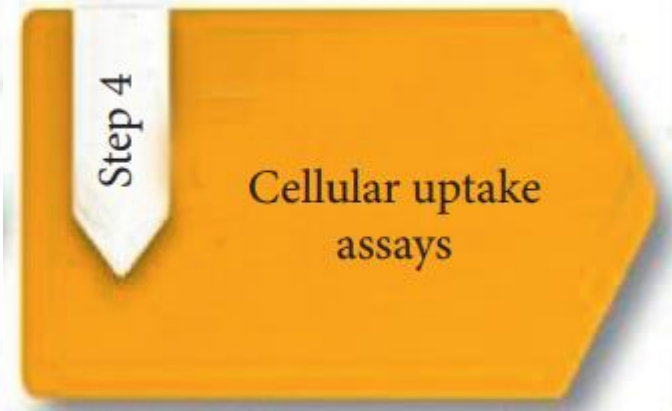
MDA-MB-231 cells were seeded at a density of  $8 \times 10^3$  per well in 96-well plates and incubated overnight at 37°C with 5% CO<sub>2</sub> in air. 0.025, 0.05, 0.1, 0.25, and 0.7 mM of SPION@ CMD and SPION@CMD@triptorelin were separately added to the culture medium and incubation was sustained for an additional 24 h. The MTT assay was performed after 48 h. the absorbance was measured at a wavelength of 545 nm with a reference wavelength of 630 nm using an ELISA reader.

## MTT Result



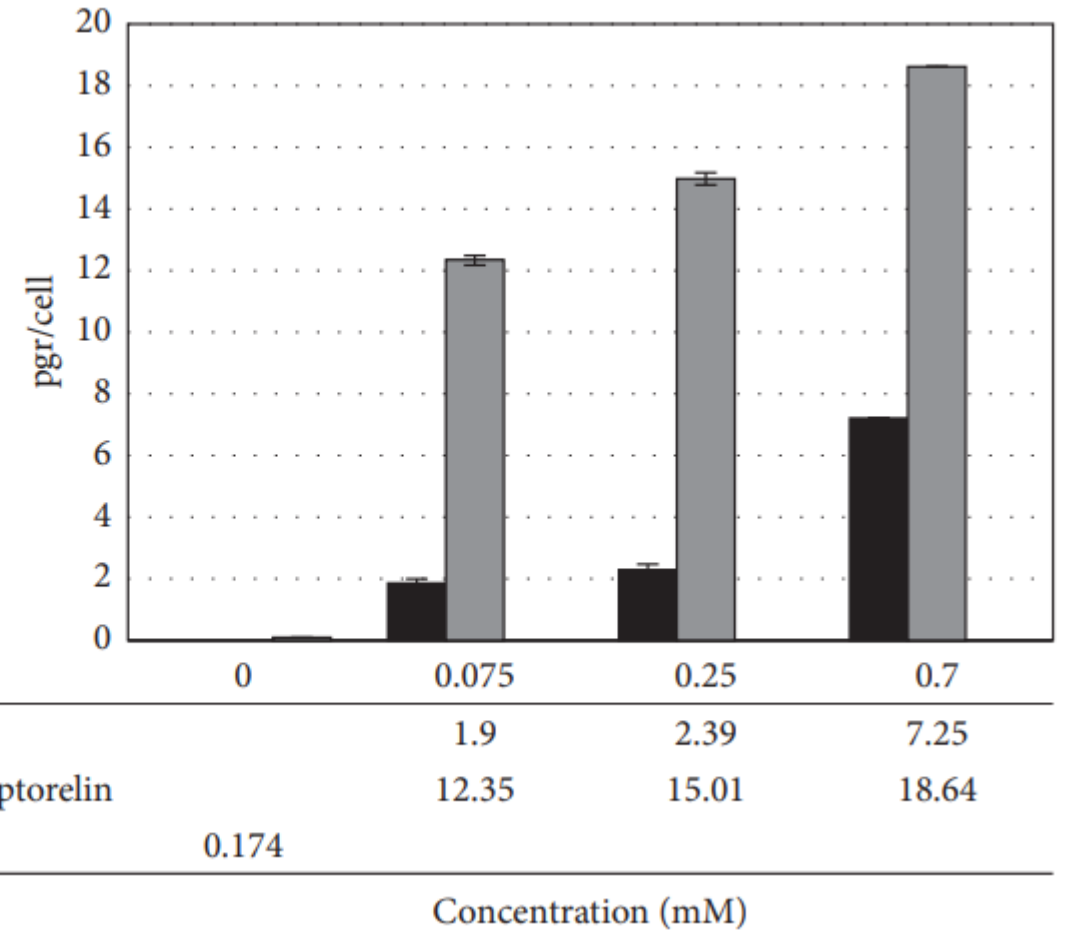
The cytotoxicity by MTT assay.

difference between cytotoxicity of SPION@CMD at concentrations of 0.025, 0.05, 0.1, 0.25, and 0.7 mM and control group was **not significant** (\* $p > 0.05$ ), while 0.7 mM SPION@CMD showed a significant difference in comparison with the control group. The test also showed a survival rate of more than 60% for the maximum concentration of 0.7 mM SPION@CMD@triptorelin . confirmed the **lack of cellular cytotoxicity of SPION@CMD@triptorelin formulation**.



## Result

The MDA-MB-231 cancer cells were seeded in 6-well plates at the density of  $4 \times 10^5$  cells/well and incubated overnight. Then incubated with 0.075, 0.25, and 0.7 mM of SPION@CMD and SPION@CMD@triptorelin for 24 h. washed three times with PBS and break down with perchloric acid. the concentration of Fe in cells was estimated with atomic absorption spectroscopy (AAS).



According to the atomic absorption spectroscopy results, the **intracellular** iron of MDA-MB-231 cells treating with **triptorelin-coated SPIONs** was **more than noncoated SPIONs**. It is confirmed that the cellular uptake efficiency of targeted SPION@CMD@triptorelin was better than SPION@CMD





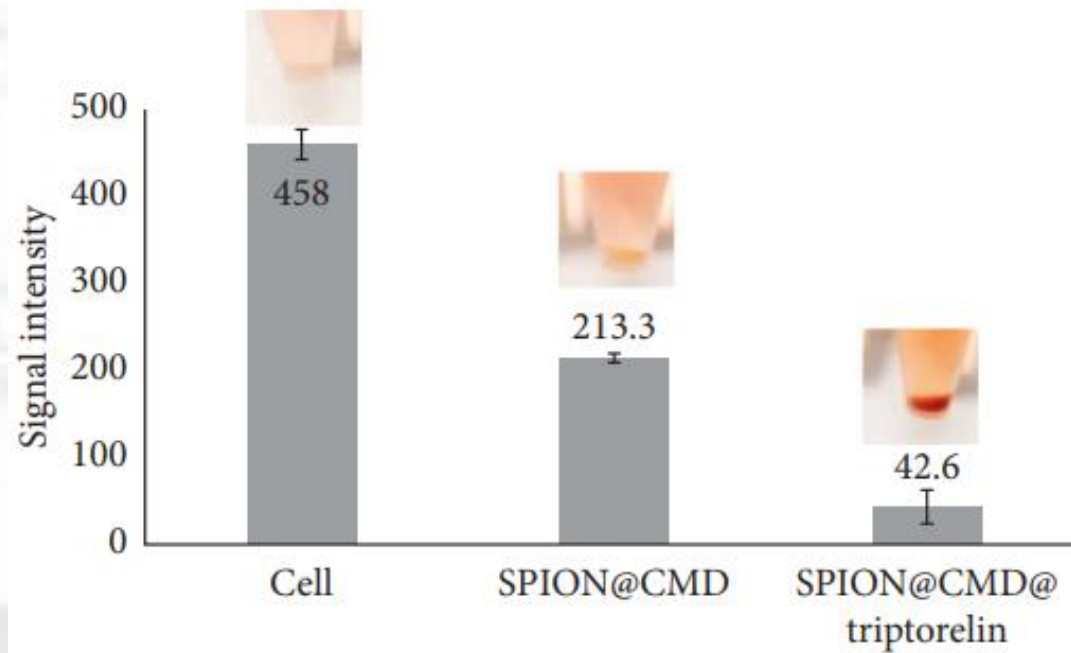
Cell

(SPION@CMD)

SPION@CMD@triptorelin

**MRI** technique was used to **visualize the accumulation** of prepared SPION@CMD and SPION@CMD@triptorelin in MDA-MB-231 cells. MDA-MB-231 cells ( $1.5 \times 10^6$ ) were seeded in T25 flasks and incubated overnight at  $37^\circ\text{C}$ . Following incubation, SPION@CMD and SPION@CMD@triptorelin with concentrations of 0.25 mM were added to each T25 flask and incubated for 24 h. the cells were washed with PBS, and  $3 \times 10^6$  cells were placed in 2 mL tubes in 0.4% agarose solution. Cells in agarose without incubation with nanoparticles were used as the control. The **T2-weighted images** were obtained using a 1.5 T MRI scanner.

SPSS was used for data analysis.



Signal intensity depended on the nanostructures (SPION@CMD and SPION@CMD@peptide).

T2-weighted MR image in cellular medium with 24-hour incubation time

The ability of the synthesized nanoparticles to targeting specifically to the MDA-MB-231 cells was also confirmed with MR imaging techniques. The results demonstrated that nanoparticles functionalized with triptorelin **reduced** by more than 90% MR image intensity compared with the 53% reduction in SPION@CMD at a Fe concentration of 0.25 mM.

Step 6

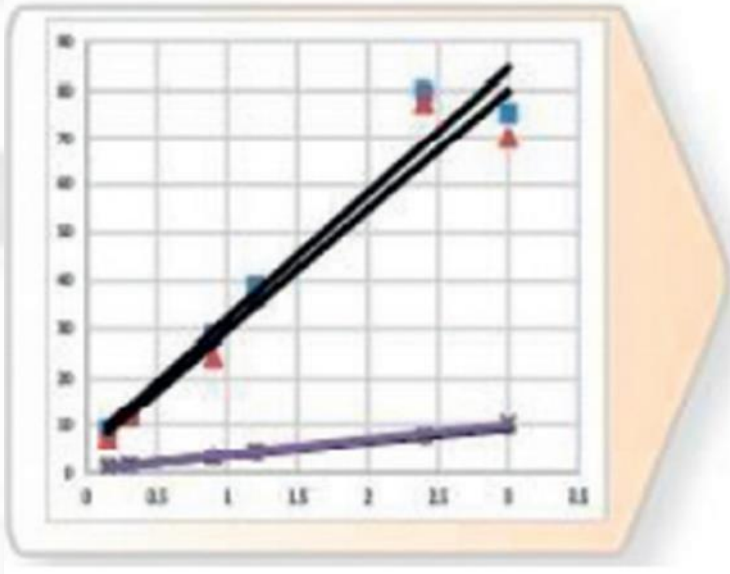
Relaxometry

**2.7. Relaxometry.** The MR capability of SPION@CMD and SPION@CMD@triptorelin was carried out based on the relaxation rates ( $R = (1/T_{1,2})$ ) which increase linearly with the SPIONs concentration according to the following equation:

$$\frac{1}{T_{1,2}} = \frac{1}{T_0} + r_{1,2}C,$$

The relaxation rate of pure water

Concentration of SPIONs





Longitudinal and transversal relaxivities' values ( $r_1$  and  $r_2$ ) were measured at 1.5 Tesla MRI scanner, using a phantom containing SPION@CMD@triptorelin with various concentrations of 0.15, 0.30, 0.9, 1.20, 2.40, and 3.0 mM.

T1 and T2-weighted images were obtained.

All curve fitting routines, which were used to determine the relaxation rate maps, were performed by Origin, Excel, and RadiAnt DICOM Viewer software.

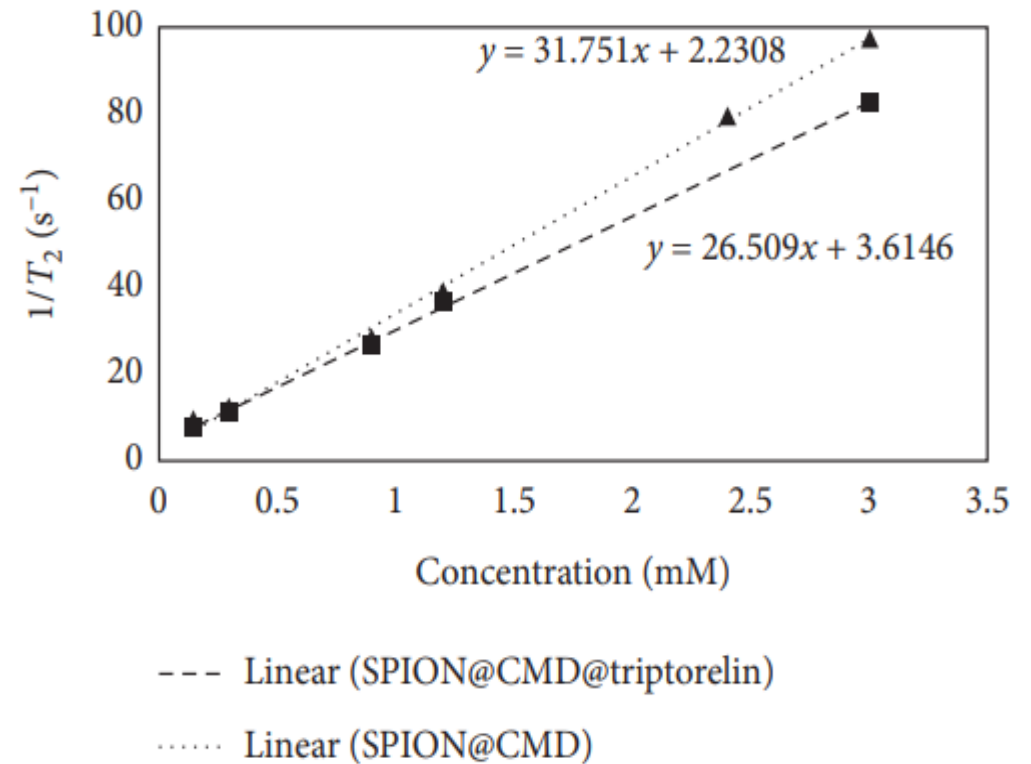
The software has the capability to open and display studies obtained from different imaging modalities:

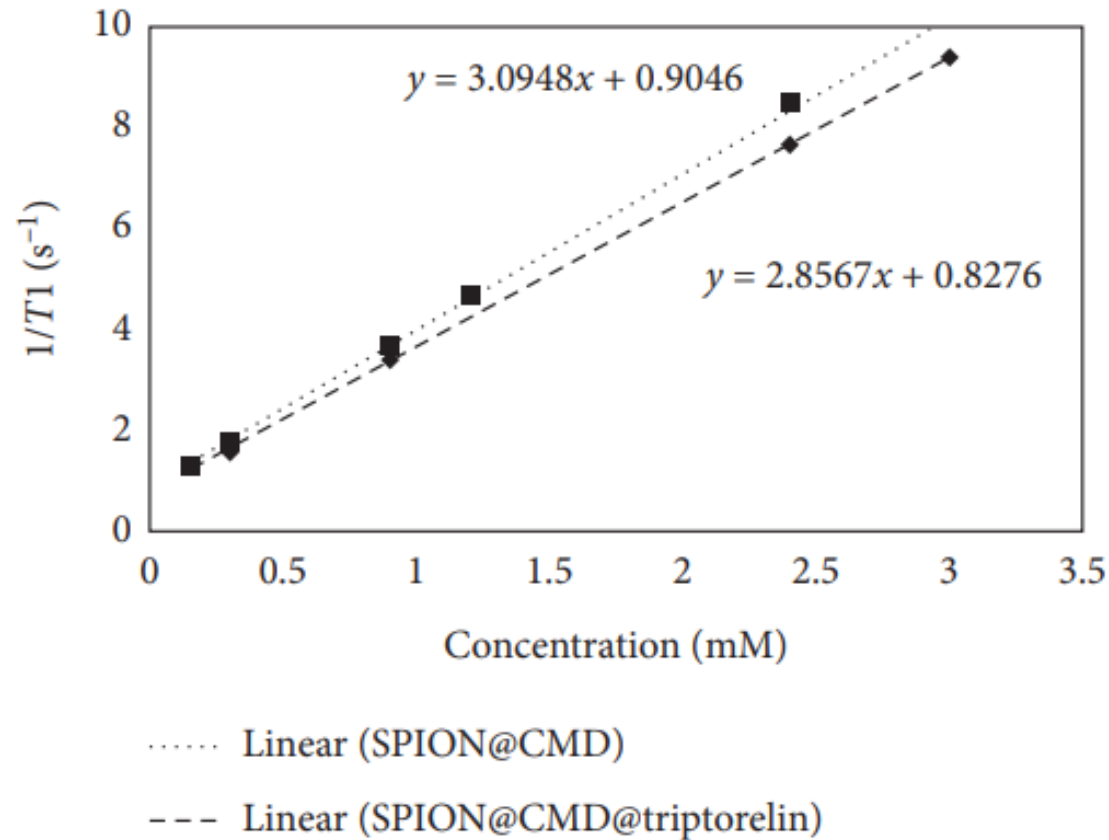
- Digital Radiography (CR, DX)
- Mammography (MG)
- Computed Tomography (CT)
- Magnetic Resonance (MR)
- Positron Emission Tomography PET-CT (PT)
- Ultrasonography (US)
- Digital Angiography (XA)
- Gamma Camera, Nuclear Medicine (NM)
- Secondary Pictures and Scanned Images (SC)
- Structured Reports (SR)



## Result

The  $r_2$  relativity was calculated as  $31.75 \text{ mM}^{-1} \text{ s}^{-1}$  according to the linear plot slope of the SPION@CMD concentration depending on the inverse  $T_2$  with  $R^2 = 0.9965$ , while the  $r_2$  relativity was obtained as  $26.51 \text{ mM}^{-1} \cdot \text{s}^{-1}$  with  $R^2 = 0.9991$  for SPION@CMD@triptorelin which was lower than SPION@CMD






Calculated **T1 relaxation rate** and **relaxivity** at various Fe concentrations of SPION@CMD and SPION@CMD@triptorelin. T1-weighted images were acquired with fix TE of 8.7 ms and TRs ranging between 100 and 2000 ms for T1 measurement at various concentrations (0.15–0.3 mM) that were prepared in the deionized water, and deionized water played a role as a control sample

# Discussion

- Targeted imaging probes is very important to improve diagnostic methods due to stability and biocompatibility.
- the main drawbacks of using SPIONs : aggregation and instability at physiological pH. To overcome these limitations, various surface coatings have been used to modify their surface properties.
- modification of SPIONs with carboxyl (-COOH) groups provide appropriate sites can be conjugated with any drugs and/or natural compounds containing amine (-NH<sub>2</sub>) group or their combinations.

- Contrast agents improve the quality of the images, but the **injectable dose** of them is limited.
- The utilization of ligands such as peptides can specifically increase the cell uptake by targeted cells → in applying lower concentration of the contrast agent.
- Recent studies have found that bare Fe<sub>3</sub>O<sub>4</sub> nanoparticles could induce the **cytotoxicity** and **apoptosis** by ROS generation and oxidative stress. (by MTT)

- The evaluation of cellular uptake of formulations on MDA-MB-231 cell line indicated the importance of **triptorelin peptide** on the **uptake** of the targeted formulation.
- all concentrations, the **cellular uptake** for SPION@CMD@ triptorelin was  SPION@CMD. (😊delivery of MRI agents with peptides increased the cellular internalization of functionalized-SPIONs in vitro)

- The mechanism of triptorelin-based internalization gives rise to **receptor-mediated endocytosis**, resulting in **efficient internalization** of formulation into the GnRH-expressing cells.
- cellular uptake of 7.25 pg/cell at the concentration of 0.7 mM (39.2 µg/ml) for the same cell line and incubation time in last study.
- the obtained average hydrodynamic diameters for SPION@CMD and SPION@CMD@triptorelin by DLS was **160 and 116 nm**.



- The TEM image showed the synthesized SPIONs had **uniform** and **heterogeneous** morphology with an average size of 31 nm, while the size **distribution histogram** obtained from TEM image revealed also that the SPIONs as low as 10–20 nm.
- The small sizes of SPION@CMD in TEM image in comparison to DLS might be the determination of the **hydrodynamic** diameter of the CMD-coated SPIONs via DLS in aqueous solution incorporating **surface-bound water layers** in their measurement, while TEM estimates the actual core size of dried SPIONs. the larger size in TEM image might be emanated from higher aggregation tendency of the **smaller SPIONs due to Van der Waals forces between the particles**.



MR images ( $T_2$ -weighted imaging) of SPION@CMD and SPION@CMD@triptorelin in an aqueous environment evaluated a noticeable contrast by changing the concentrations of SPIONs. Therefore, SPION@CMD@triptorelin could be considered as a targeted negative contrast agent. The  $r_2$  value of SPION@CMD and SPION@CMD@triptorelin was estimated at  $31.75 \text{ mM}^{-1} \cdot \text{s}^{-1}$  and  $26.50 \text{ mM}^{-1} \cdot \text{s}^{-1}$ , respectively, by a magnetic relaxometry at a 1.5 T conventional MRI system. The size, mass magnetization ( $M_s$ ), and the magnetic field strength are factors affect the  $r_2$  value [38, 39]. In agreement with previous studies, the obtained  $r_2$  indicated that  $T_2$  relativity also depends on the concentration of SPIONs. It was also demonstrated that the large sizes of SPIONs and stronger magnetic field lead to the higher  $r_2/r_1$ . The high value of  $r_2/r_1$  ratio indicated  $T_2$  contrast agent [40, 41]. In the present study, the calculated  $r_2/r_1$  indicated SPION@CMD@triptorelin as a good candidate for a negative contrast agent in clinical magnetic field strength.

# Conclusion

## In the present study

SPION@CMD@triptorelin  
, as a **targeted probe in  
GnRH + cancer cells**,  
synthesized by a  
coprecipitation method and  
size of  
**31 nm**

$T_2$  relaxivities ( $r_2$ ) were  
determined to be **31.75**  
 $\text{mM}^{-1} \cdot \text{s}^{-1}$  for  
**SPION@CMD** and **26.50**  
 $\text{mM}^{-1} \cdot \text{s}^{-1}$  for  
**SPION@CMD@triptorelin**

in vitro cell viability  
assays:  
SPION@CMD@triptorelin  
showed **no cellular**  
**viability reduction** for up  
to 0.7 mM

- The findings suggested that **SPION@CMD@triptorelin** can be used in the future **as a targeted theranostic agent** for improving diagnostic and therapeutic application.
- It can be concluded that **SPION@CMD@triptorelin** loaded with anticancer drug provides **a theranostic platform** for specific delivery of MRI agents and drugs

## References

- [1] F. Bray, J. Ferlay, I. Soerjomataram, R. L. Siegel, L. A. Torre, and A. Jemal, "Global cancer statistics 2018: GLOBOCAN estimates of incidence and mortality worldwide for 36 cancers in 185 countries," *CA: A Cancer Journal for Clinicians*, vol. 68, no. 6, pp. 394–424, 2018.
- [2] K. D. Miller, A. Goding Sauer, A. P. Ortiz et al., "Cancer statistics for hispanics/latinos, 2018," *CA: A Cancer Journal for Clinicians*, vol. 68, no. 6, pp. 425–445, 2018.
- [3] R. A. Smith, K. S. Andrews, D. Brooks et al., "Cancer screening in the United States, 2018: a review of current American cancer society guidelines and current issues in cancer screening," *CA: A Cancer Journal for Clinicians*, vol. 68, no. 4, pp. 297–316, 2018.
- [4] C. Li, Y. Meng, S. Wang et al., "Mesoporous carbon nanospheres featured fluorescent aptasensor for multiple diagnosis of cancer in vitro and in vivo," *ACS Nano*, vol. 9, no. 12, pp. 12096–12103, 2015.
- [5] R. L. Siegel, K. D. Miller, and A. Jemal, "Cancer statistics, 2015," *CA: A Cancer Journal for Clinicians*, vol. 65, no. 1, pp. 5–29, 2015.
- [6] A. Montazerabadi, J. Beik, R. Irajirad et al., "Folate-modified and curcumin-loaded dendritic magnetite nanocarriers for the targeted thermo-chemotherapy of cancer cells," *Artificial Cells, Nanomedicine, and Biotechnology*, vol. 47, no. 1, pp. 330–340, 2019.
- [7] L. Fass, "Imaging and cancer: a review," *Molecular Oncology*, vol. 2, no. 2, pp. 115–152, 2008.
- [8] J. V. Frangioni, "New technologies for human cancer imaging," *Journal of Clinical Oncology*, vol. 26, pp. 4012–4021, 2008.
- [9] J. Dulińska-Litewka, A. Łazarczyk, P. Hałubiec, O. Szafranski, K. Karnas, and A. Karewicz, "Superparamagnetic iron oxide nanoparticles-current and prospective medical applications," *Materials*, vol. 12, no. 4, p. 617, 2019.
- [10] R. Revia and M. Zhang, "Magnetite nanoparticles for cancer diagnosis, treatment, and treatment monitoring: recent advances," *Mater Today (Kidlington)*, vol. 19, no. 3, pp. 157–168, 2016.
- [11] E. Doolittle, P. M. Peiris, G. Doron et al., "Spatiotemporal targeting of a dual-ligand nanoparticle to cancer metastasis," *ACS Nano*, vol. 9, no. 8, pp. 8012–8021, 2015.
- [12] A. Singh and S. K. Sahoo, "Magnetic nanoparticles: a novel platform for cancer theranostics," *Drug Discovery Today*, vol. 19, no. 4, pp. 474–481, 2014.



- [13] A. R. Montazerabadi, M. A. Oghabian, R. Irajirad et al., "Development of gold-coated magnetic nanoparticles as a potential MRI contrast agent," *Nano*, vol. 10, no. 4, p. 1550048, 2015.
- [14] M. S. Jabir, U. M. Nayef, W. K. Abdulkadhim, and G. M. Sulaiman, "Supermagnetic Fe<sub>3</sub>O<sub>4</sub>-PEG nanoparticles combined with NIR laser and alternating magnetic field as potent anti-cancer agent against human ovarian cancer cells," *Materials Research Express*, vol. 6, no. 11, p. 115412, 2019.
- [15] L. Shen, B. Li, and Y. Qiao, "Fe<sub>3</sub>O<sub>4</sub> nanoparticles in targeted drug/gene delivery systems," *Materials*, vol. 11, no. 2, p. 324, 2018.
- [16] Wahajuddin and S. Arora, "Superparamagnetic iron oxide nanoparticles: magnetic nanoplatforms as drug carriers," *International Journal of Nanomedicine*, vol. 7, pp. 3445–3471, 2012.
- [17] C. Chandola and M. Neerathilingam, "Aptamers for targeted delivery: current challenges and future opportunities," *Role of Novel Drug Delivery Vehicles in Nanobiomedicine*, IntechOpen, London, UK, 2019.
- [18] S. Yoon and J. J. Rossi, "Aptamers: uptake mechanisms and intracellular applications," *Advanced Drug Delivery Reviews*, vol. 134, pp. 22–35, 2018.
- [19] H. Cakmak and M. P. Rosen, "Current clinical approaches to protecting the ovary: GnRH analogues," in *Cancer Treatment and the Ovary: Clinical and Laboratory Analysis of Ovarian Toxicity* Academic Press, Cambridge, MA, USA, 2015.
- [20] A. S. Merseburger and M. C. Hupe, "An update on triptorelin: current thinking on androgen deprivation therapy for prostate cancer," *Advances in Therapy*, vol. 33, no. 7, pp. 1072–1093, 2016.
- [21] S. Albukhaty, S. Al-Musawi, S. Abdul Mahdi et al., "Investigation of dextran-coated superparamagnetic nanoparticles for targeted vinblastine controlled release, delivery, apoptosis induction, and gene expression in pancreatic cancer cells," *Molecules*, vol. 25, no. 20, p. 4721, 2020.
- [22] M. Serhan, M. Sprowls, D. Jackemeyer et al., "Total iron measurement in human serum with a smartphone," in *Proceedings of the AIChE Annual Meeting*, Orlando, FL, USA, November, 2019.
- [23] S. C. Hong, J. H. Lee, J. Lee et al., "Subtle cytotoxicity and genotoxicity differences in superparamagnetic iron oxide nanoparticles coated with various functional groups," *International Journal of Nanomedicine*, vol. 6, pp. 3219–3231, 2011.
- [24] H. Singh, J. Du, P. Singh, G. T. Mavlonov, and T. H. Yi, "Development of superparamagnetic iron oxide nanoparticles via direct conjugation with ginsenosides and its in-vitro study," *Journal of Photochemistry and Photobiology B*, vol. 185, pp. 100–110, 2018.
- [25] Z. Hu, H. Zhang, Y. Zhang, R. Wu, and H. Zou, "Nanoparticle size matters in the formation of plasma protein coronas on Fe<sub>3</sub>O<sub>4</sub> nanoparticles," *Colloids and Surfaces B: Biointerfaces*, vol. 121, pp. 354–361, 2014.
- [26] M. S. Jabir, U. M. Nayef, W. K. Abdulkadhim et al., "Fe<sub>3</sub>O<sub>4</sub> nanoparticles capped with PEG induce apoptosis in breast cancer AMJ13 cells via mitochondrial damage and reduction of NF- $\kappa$ B translocation," *Journal of Inorganic and Organometallic Polymers and Materials*, vol. 31, no. 3, pp. 1241–1259, 2020.

- [27] Y.-D. Xiao, R. Paudel, J. Liu, C. Ma, Z.-S. Zhang, and S.-K. Zhou, "MRI contrast agents: classification and application," *International Journal of Molecular Medicine*, vol. 38, no. 5, pp. 1319–1326, 2016.
- [28] N. Nitin, L. E. W. LaConte, O. Zurkiya, X. Hu, and G. Bao, "Functionalization and peptide-based delivery of magnetic nanoparticles as an intracellular MRI contrast agent," *Journal of Biological Inorganic Chemistry*, vol. 9, no. 6, pp. 706–712, 2004.
- [29] J. Poller, J. Zaloga, E. Schreiber et al., "Selection of potential iron oxide nanoparticles for breast cancer treatment based on in vitro cytotoxicity and cellular uptake," *International Journal of Nanomedicine*, vol. 12, pp. 3207–3220, 2017.
- [30] M. Calero, M. Chiappi, A. Lazaro-Carrillo et al., "Characterization of interaction of magnetic nanoparticles with breast cancer cells," *Journal of Nanobiotechnology*, vol. 13, no. 1, pp. 1–15, 2015.
- [31] R. Thomas, I. K. Park, and Y. Y. Jeong, "Magnetic iron oxide nanoparticles for multimodal imaging and therapy of cancer," *International Journal of Molecular Sciences*, vol. 14, pp. 15910–15930, 2013.
- [32] D. F. de Queiroz, E. R. de Camargo, and M. A. U. Martinez, "Synthesis and characterization of magnetic nanoparticles of cobalt ferrite coated with silica," *Biointerface Research in Applied Chemistry*, vol. 10, no. 1, pp. 4908–4913, 2020.
- [33] T. Ishizaki, K. Yatsugi, and K. Akedo, "Effect of particle size on the magnetic properties of Ni nanoparticles synthesized with trioctylphosphine as the capping agent," *Nanomaterials*, vol. 6, no. 9, p. 172, 2016.
- [34] T. Theivasanthi and M. Alagar, "Innovation of superparamagnetism in lead nanoparticles," *Physics and Technical Sciences*, vol. 1, no. 3, p. 39, 2013.
- [35] H. Fattahi, S. Laurent, F. Liu, N. Arsalani, L. V. Elst, and R. N. Muller, "Magnetoliposomes as multimodal contrast agents for molecular imaging and cancer nanotheragnostics," *Nanomedicine*, vol. 6, no. 3, pp. 529–544, 2011.
- [36] M. Menelaou, Z. Iatridi, I. Tsougos, K. Vasiou, C. Dendrinou-Samara, and G. Bokias, "Magnetic colloidal superparticles of Co, Mn and Ni ferrite featured with comb-type and/or linear amphiphilic polyelectrolytes; NMR and MRI relaxometry," *Dalton Transactions*, vol. 44, no. 24, pp. 10980–10990, 2015.
- [37] Z. Mohammadi, N. Attaran, A. Sazgarnia, S. A. M. Shaegh, and A. Montazerabadi, "Superparamagnetic cobalt ferrite nanoparticles as  $T_2$  contrast agent in MRI: in vitro study," *IET Nanobiotechnology*, vol. 14, no. 5, pp. 396–404, 2020.
- [38] Y.-W. Jun, Y.-M. Huh, J.-S. Choi et al., "Nanoscale size effect of magnetic nanocrystals and their utilization for cancer diagnosis via magnetic resonance imaging," *Journal of the American Chemical Society*, vol. 127, no. 16, pp. 5732–5733, 2005.
- [39] J. Kang, H. Lee, Y. N. Kim et al., "Size-regulated group separation of  $\text{CoFe}_2\text{O}_4$  nanoparticles using centrifuge and their magnetic resonance contrast properties," *Nanoscale Research Letters*, vol. 8, no. 1, pp. 1–7, 2013.
- [40] B. Issa, I. M. Obaidat, B. A. Albiss, and Y. Haik, "Magnetic nanoparticles: surface effects and properties related to biomedicine applications," *International Journal of Molecular Sciences*, vol. 14, pp. 21266–21305, 2013.
- [41] A.-L. Rollet, S. Neveu, P. Porion, V. Dupuis, N. Cherrak, and P. Levitz, "New approach for understanding experimental NMR relaxivity properties of magnetic nanoparticles: focus on cobalt ferrite," *Physical Chemistry Chemical Physics*, vol. 18, pp. 32981–32991, 2016.





*Thanks for  
your attention*





**ANSWER**

**ASK**